Ideal torsional strengths and stiffnesses of carbon nanotubes

Elif Ertekin and D. C. Chrzan*
Department of Materials Science and Engineering, University of California, Berkeley, California 94720, USA
Materials Sciences Division, Lawrence Berkeley National Laboratory, Berkeley, California 94720, USA
(Received 6 April 2005; published 14 July 2005)

The ideal torsional strengths of a class of carbon nanotubes, and the torsional stiffnesses of *all* carbon nanotubes are computed using a novel combination of an *ab initio* electronic structure total energy technique and a physically motivated scaling form. The specific torsional strengths of multi-walled tubes are predicted to exceed those of steel by approximately a factor of 20. Closed-form expressions that bound the torsional stiffnesses are also presented. The predictions of the theory give excellent agreement with available experimental data.

DOI: 10.1103/PhysRevB.72.045425 PACS number(s): 61.50.Ah, 62.25.+g, 81.05.Tp, 81.07.De

I. INTRODUCTION

Carbon nanotubes (CNs) are particularly promising nanostructures for technological applications. Recently, a variety of CN electronic and mechanical devices have been developed, including junctions,[1] emitters,[2] nanomechanical resonators,[3] and even the world's tiniest electric motor.[4] The two latter applications employ the torsional properties of multi- and single-walled carbon nanotubes (MWNTs and SWNTs). For the resonators, the tubes act as torsional springs while for the electric motor, the tube acts as a rotational bearing.[5] Presumably, CNs will also serve as the drive shaft for the electric motor, and be used to drive other nanomechanical systems. These applications motivate the questions "How much torque can be exerted by a carbon nanotube?" and "How much can one twist a carbon nanotube before it becomes unstable?" To answer these questions, we have computed the ideal torsional strength (ITS) of a class of CNs using an electronic structure-based total energy method and a physically motivated scaling form. While the ITSs are computed for multi- and single-walled *zig-zag* carbon nanotubes (nanotubes with chirality indices $(n,0)$), we have determined from our analysis expressions for the limits of the linear torsional stiffness of *all* multi- and single-walled carbon nanotubes. The theoretical predictions correspond well to the available experimental data.

The ITS of a CN is defined here as the maximum torque that a CN can withstand given that one suppresses both the production of defects (e.g., Stone-Wales defects[6]) and any type of buckling instability.[7] The ideal strength is the inherent strength of a material; it represents the degree to which the material, free of any defects, can withstand mechanical loading before an elastic instability is induced. Ideal strength calculations provide absolute engineering bounds for material properties, and thus serve as guideposts in the development of new nanoscale mechanical structures. The computation of similar quantities, such as the ideal tensile and shear strengths of crystalline materials, has provided insight into the results of nanoindentation experiments,[8] as well as offered an explanation for the inherent brittleness of FeAl.[9] In the bulk, the computed stresses are not observed (since no material is perfect), but a notable result of these prior studies is that at the nanoscale, materials may resist plastic deformation until stresses approach these computed values.[8,10,11]

In the next section, the approach used to compute the ideal torsional strengths and the linear torsional stiffnesses of carbon nanotubes is described. The calculated stiffnesses are compared favorably with experiment, and the ideal torsional strengths compared with those of typical structural materials and with the torques exerted on biological rotors.

II. METHODOLOGY AND RESULTS

A. Ideal torsional strength

1. Single-walled carbon nanotubes

In principle, the computation of the ITS of a SWNT with total energy electronic structure methods is straightforward. One simply computes the torque T_s required to twist uniformly the tube as a function of the twist rate θ/d (while constraining the tube against buckling, etc.). The maximum torque is the ITS. In practice, however, the computation is a bit more involved. Figure 1 illustrates how the lattice of a typical zig-zag CN is deformed in response to an applied twist. The axis of rotation (that coincides with the nanotube axis) is along the z direction of a cylindrical coordinate system. The twist angle coincides with the coordinate θ, while the length of the tube is given by d. In the untwisted form (Fig. 1(a)), the structure of the tube is periodic in the z direction with a small period. This periodicity can be exploited to reduce the number of atoms involved in the calculation. As the tube twists (Fig. 1(b)), the periodicity in the z direction is altered. For many values of the twist rate θ/d (Fig. 1(c)), the structure of the tube is no longer periodic in z, and the calculation of the total energy becomes intractable. However, for special values of the twist angle, the twisted tube retains its periodicity and the calculation of the total energy becomes tractable, provided the number of atoms is not too large (for the resources available to us, fewer than 450 carbon atoms). Through judicious choices of twist angles, one can compute the functional dependence of total energy density E/d on the twist rate θ/d for a given $(n,0)$ nanotube. From this, the torque is easily obtained from the expression

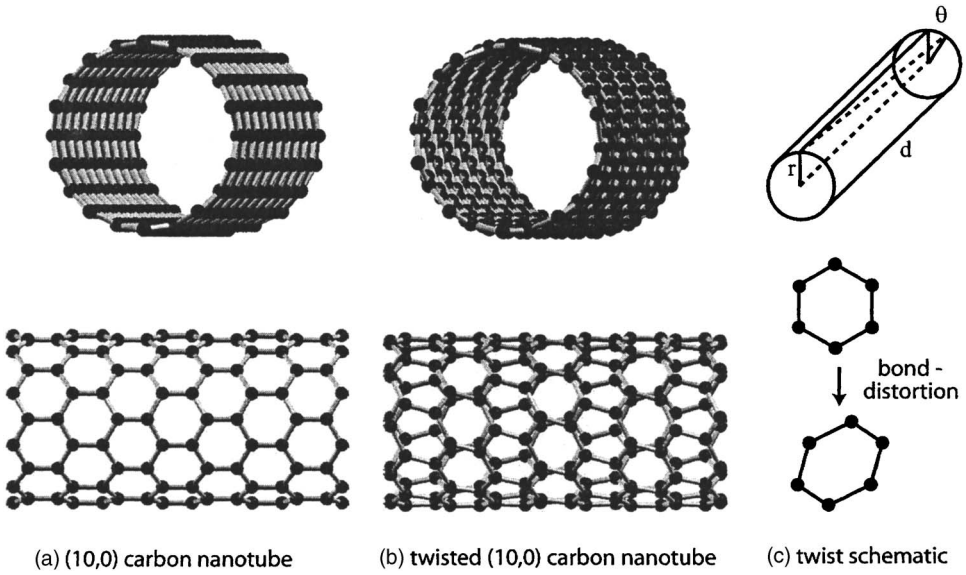

FIG. 1. The studied SWNTs. (a) Untwisted (10,0) CN viewed both along its axis and perpendicularly. (b) The same nanotube, but twisted uniformly. (c) The twisting distorts the carbon hexagons as shown.

$$T_s = \frac{d(E/d)}{d(\theta/d)}. \tag{1}$$

The total energy electronic structure calculations presented here employ the formalism embodied in the *Vienna Ab-Initio Simulation Package* (VASP),[12,13] relying on the local density approximation to density functional theory, and ultrasoft pseudopotentials with a cutoff energy of 211 eV. A tetragonal supercell consisting of one repeating period and typically containing 300–450 carbon atoms (e.g., Fig. 1) was used for all of the twisted and untwisted states sampled. The spacing between carbon nanotubes was greater than 10 Å to avoid image interactions between the tubes. For structural relaxation, a single k point located at $\Lambda=(1/2,1/2,1/2)$ in the Brillouin zone was found to be sufficient. For the twisted tubes, one of the two atoms of the graphene unit cell was fixed by the applied twist, while the other atom was permitted to fully relax. With these parameters, the total energy is converged to within 1 mRy/atom.

The computed torque T_s versus twist rate θ/d curves for zig-zag nanotubes, with $n=10$, 14, and 18, are displayed in Fig. 2(a). The maximum torque in each of the curves corresponds to the onset of the instability, and hence represents the ITS of the CN. These curves reveal important trends. The most obvious trend is that the torsional stiffnesses and ITSs of the tubes increase with radius; the second most obvious trend is that the curves all have similar shapes.

Both of these trends are consistent with a simple physical picture that allows one to extrapolate the present results to predict the ITS of *any* zig-zag SWNT. Within the geometry of the nanotube, the torsional force is largely due to the bending of the bonds under twist (Figs. 1(b) and 1(c)). As the nanotube is twisted, the graphitically bonded hexagons in the nanotube are sheared. The degree of shear increases with twist rate θ/d. Based on the geometry, the shear is a function of $r\theta/d$ with r the radius of the tube. The amount of material sheared is simply proportional to the circumference of the tube. If one assumes that the restoring force (under ideal torsion) depends only on this shear, one concludes that the torque T_s exerted by a twisted zig-zag tube will depend on the radius of the tube according to

$$T_s = r^2 f\left(r\frac{\theta}{d}\right), \tag{2}$$

where $f(r\theta/d)$ is proportional to the shear force. Equation (2) suggests that a plot of T_s/r^2 versus $r\theta/d$ for various values of r will yield one curve, independent of r. The ITS then is given by $r^2 f_{max}$, where f_{max} is the maximum of $f(r\theta/d)$.

Figure 2(b) displays the data of Fig. 2(a) plotted as suggested by Eq. (2), thus effectively plotting $f(r\theta/d)$. The data collapse is quite good, suggesting that the form of Eq. (2) is robust. We have computed as well the energy to shear (in a corresponding manner as shown in Fig. 1(c)) a rectangular

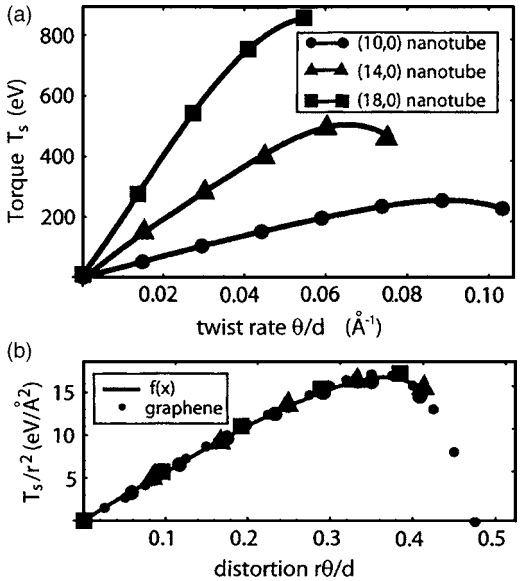

FIG. 2. (a) Torque T_s as a function of twist rate θ/d computed using the total energy technique described in the text for different zig-zag nanotubes. (b) T_s/r^2 vs $r\theta/d$ plotted, as suggested by Eq. (2). The collapse of the curves suggests that Eq. (2) is a good description of the torsional strength of zig-zag nanotubes. The solid line is a sixth-order polynomial fit to the scaled data used to represent $f(x)$.

graphene layer of dimensions $(2\pi r)\times(d)=A$ oriented so that d represents the same direction in the nanotubes and the graphene. For graphene, we plot in Fig. 2(b) the corresponding quantity $2\pi d(E/A)/d(r\theta/d)$ vs $r\theta/d$, which collapses onto the same scaled curve. This illustrates that the torque exerted by a twisted carbon nanotube is described well by considering the energy required to shear a graphene layer in a corresponding manner.

2. Multi-walled carbon nanotubes

The ITSs of MWNTs are not simply obtained by direct computation using *ab initio* electronic structure total energy methods. The number of atoms increases substantially and the calculation quickly becomes too expensive. The method used here relies instead on the fact that interwall interactions for (undeformed) CNs are known to be weak[5,14] and that the ITS of a SWNT is governed by the scaling form represented in Eq. (2). Given these observations, the torque exerted by a MWNT may be written as the sum of the torques exerted by each of the individual tubes comprising the MWNT. For simplicity, we assume that the twist angle θ is fixed, and equal, for each tube. The total torque T_m exerted by the MWNT for a given twist rate θ/d is

$$T_m=\sum_{r=r_{inner}}^{r_{outer}} r^2 f(r\theta/d), \tag{3}$$

where r_{outer} is the outer radius of the MWNT and r_{inner} is the corresponding inner radius. To compute the ITS of a MWNT, Eq. (3) should be evaluated at the twist rate θ/d for which the most exterior tube just reaches the maximum in the function $f(r_{outer}\theta/d)$, approximately at $r_{outer}\theta/d=0.366$. A further increase in twist will drive the outermost nanotube to failure, and the transfer of load to the interior tubes will be enough to drive the remaining tubes to their point of instability, leading to failure of the entire MWNT. The ITS thus computed is the ideal torsional strength of the MWNT.

It is interesting to compare the ITS of a MWNT to that of a solid nanorod of a traditional structural material. The ITSs must be compared for the two systems at the same size scale. Therefore, the individual nanotubes comprising the MWNT are chosen so that it is maximally nested with CNs with intertube spacing of $\approx$3.5 Å, roughly the interplanar spacing in graphite. Figure 3 displays the ultimate torsional strength of a carbon nanotube as a function of radius. For the zig-zag MWNTs considered here, the chiral vectors $(n,0)$ of the nested tubes have $n=9,18,27,\ldots,9N$ with N the total number of tubes in the MWNT. Figure 3 also displays the same quantity computed for an iron rod of the same radius. (This curve was constructed using the ideal stress versus strain curve for Fe, using the ideal shear stress of 7.2 GPa along $\langle 112\rangle$ $\{112\}$.[15]) The ITS of the MWNT exceeds that of the equivalent Fe rod for all finite radii rods by (approximately) a factor of 20. Since the ideal strength of Fe and steel should not be too different—the primary component of steel is Fe—this plot indicates that the carbon nanocrankshaft has the potential to be substantially stronger than its steel equivalent.

Nevertheless, the ITS values are quite small. It is interesting, however, to compare the values computed here to those exerted by one of nature's similar components: a bacterial flagella motor. The torque produced by a typical bacterial flagella motor is around 25 eV, and acts on a tube with a radius of approximately 20 nm.[16] The ITS of a carbon nanotube is, in contrast, approximately 400 000 times larger. Even if one includes a factor of 10 000 reduction in strength for the introduction of defects, the nanotube can withstand roughly 40 times the torque exerted by a typical bacterial motor. Thus MWNTs display remarkable torsional strength.

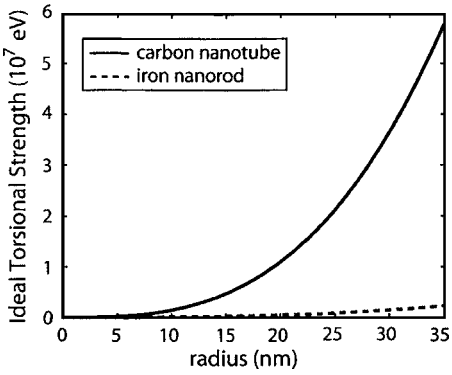

FIG. 3. The ITS of a MWNT compared with a Fe rod of the same dimensions. The MWNTs are roughly 20 times stronger than an iron rod of the same size.

B. Linear torsional stiffnesses

Equations (2) and (3) can be used to compute the linear torsional stiffnesses K_s of SWNTs and K_m of MWNTs, respectively. Defining the torsional stiffnesses by the relationships $T_s=K_s\theta$ and $T_m=K_m\theta$, expanding Eq. (3) to first order in θ and then performing the summation, yields

$$K_m=\frac{1}{4}\left(\frac{9\sqrt{3}}{2\pi}\right)^3\frac{a^3}{d}N^2(1+N)^2f'(0) \tag{4}$$

and

$$K_s=\frac{r^3}{d}f'(0), \tag{5}$$

where the first relationship is valid for the maximally nested MWNTs, as before. Here, a is 1.42 Å (the carbon-carbon spacing in graphite), $f'(0)$ is the slope of the scaling function plotted in Fig. 2(b) at $r\theta/d=0$, evaluated numerically to be 58 ± 6 eV/Å^2, and d is the length of the tube. (An error margin of roughly 10% accounts both for numerical errors as well as the LDA's overestimate of the elastic constants.) We have used the geometric relationship $na\sqrt{3}=2\pi r$, which holds for zig-zag nanotubes with large r. Note that for large N the stiffness K_m scales with N^4, a result expected from classical elasticity theory.

These predicted stiffnesses, though derived from calculations based on zig-zag nanotubes, are more broadly applicable. The underlying assumption of the above expressions is that the shear properties of the graphitic sheets of carbon determine the torsional stiffness. These graphitic sheets are elastically isotropic, and consequently the torsional stiffness

of *any* (n,m) CN should be described well by Eq. (5). Similarly, Eq. (4) should describe the linear stiffnesses of all MWNTs, to the extent that the nesting of the nanotubes is reflected properly.

Equations (4) and (5) place bounds on the stiffness of MWNTs that can be compared with experimental measurements. Experimental estimates of the torsional stiffness of MWNTs have been obtained by various authors.[3,4,17] Typical tube diameters range from 12 to 36 nm. In the experiments, the nesting structure of the MWNTs and the degree to which all tubes are twisted during the measurement is unknown. However, the extremes are well defined: at least the largest radius nanotube must be twisted to the measured angle, and at most all tubes in a maximally nested MWNT are twisted to the measured angle. Thus the torsional stiffness of the tube must fall roughly between that for the outermost single-walled nanotube (Eq. (5) with $r=r_{outer}$) and the case of all nanotubes perfectly coupled (Eq. (4)).

In Fig. 4 we compare the torsional spring constants obtained by Refs. 3 and 17 to those obtained with Eqs. (4) and (5) using $f'(0)=58$ eV/Å^2. Note that we consider the intrinsic torsional stiffness of the nanotubes κ, where $T_m=\kappa_m\theta/d$ and $T_s=\kappa_s\theta/d$. We have also placed error bars on the experimental measurements, which arise from the 20% uncertainty in the measurement of the radii reported by Williams *et al.*[17] and Papadakis *et al.*[3] With the exception of only two data points from Ref. 17, when these error bars are included, all of the experimental measurements fall within the bounds of our theory. It should be noted that the theory has no adjustable parameters and, therefore, the agreement with experiment is quite remarkable. Additionally, authors Williams *et al.*[17] note that for a given CN, the measured stiffness increases with subsequent experiments and suggest that this can be explained by considering that with each measurement, more of the nested tubes becomes coupled to the paddle and are twisted. It is also possible that the interlayer coupling may be increasing as a result of defect formation, resulting in some form of strain hardening—a possibility that has not been incorporated in our theory.

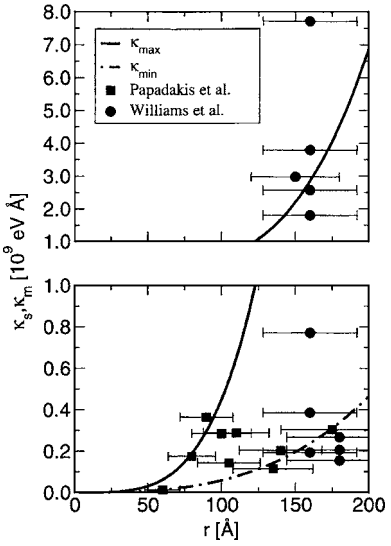

FIG. 4. A comparison of experimentally measured intrinsic torsional stiffness and the theoretical predictions for zig-zag MWNTs. The solid and dashed lines give, respectively, the maximum and minimum stiffnesses predicted by the theory. The fact that some of the measured stiffnesses exceed those predicted by the theory can be attributed to uncertainty in the measured nanotube radii and possibly to enhanced interwall interactions that may enhance the stiffness.

III. CONCLUSIONS

In conclusion, it is demonstrated the stiffnesses and ITS of many CNs can be described quite well by extrapolating from the properties of a single graphene sheet. The bounds on torsional stiffnesses so predicted agree very well with available experimental data, considering that the theory employs no adjustable parameters. Predicted values for the ITS exceed those of Fe by approximately a factor of 20, and the torque exerted by a typical bacterial motor by a factor of 400 000.

ACKNOWLEDGMENTS

EE acknowledges the support of the Intel Corporation. DCC acknowledges the support of the Miller Institute for Basic Science Research. This research was supported in part by the Department of Energy, Basic Energy Sciences under the Office of Science under Contract No. DE-AC02-05CH11231, and, in part, by the National Science Foundation under Contract No. DMR-0304629.

*Electronic address: dcchrzan@berkeley.edu

[1] M. S. Fuhrer, J. Nygard, L. Shih, M. Forero, Y.-G. Yoon, M. S. C. Mazzoni, H. J. Choi, J. Ihm, S. G. Louie, and A. Zettl, Science **288**, 497 (2000).

[2] N. D. Jonge and J.-M. Bonard, Philos. Trans. R. Soc. London, Ser. A **362**, 2239 (2004).

[3] S. J. Papadakis, A. R. Hall, P. A. Williams, L. Vicci, M. R. Falvo, R. Superfine, and S. Washburn, Phys. Rev. Lett. **93**, 146101 (2004).

[4] A. M. Fennimore, T. D. Yuzvinsky, W.-Q. Han, M. S. Fuhrer, J. Cumings, and A. Zettl, Nature (London) **424**, 408 (2003).

[5] A. N. Kolmogorov and V. H. Crespi, Phys. Rev. Lett. **85**, 4727 (2000).

[6] M. B. Nardelli, B. I. Yakobson, and J. Bernholc, Phys. Rev. Lett. **81**, 4656 (1998).

[7] B. I. Yakobson, C. J. Brabec, and J. Bernholc, Phys. Rev. Lett. **76**, 2511 (1996).

[8] C. R. Krenn, D. Roundy, M. L. Cohen, D. C. Chrzan, and J. W. Morris, Jr., Phys. Rev. B **65**, 134111 (2002).

[9] T. Li, J. W. Morris, Jr., and D. C. Chrzan, Phys. Rev. B **70**,

054107 (2004).
[10] D. Roundy, C. R. Krenn, M. L. Cohen, and J. W. Morris, Jr., Phys. Rev. Lett. **82**, 2713 (1999).
[11] A. Gouldstone, H.-J. Koh, K.-Y. Zeng, A. E. Giannakopolous, and S. Suresh, Acta Mater. **48**, 2277 (2000).
[12] G. Kresse and J. Fürthmuller, Phys. Rev. B **54**, 11169 (1996).
[13] G. Kresse and J. Fürthmuller, Comput. Mater. Sci. **6**, 15 (1996).
[14] J. P. Lu, Phys. Rev. Lett. **79**, 1297 (1997).
[15] D. M. Clatterbuck, D. C. Chrzan, and J. W. J. Morris, Acta Mater. **51**, 2271 (2003).
[16] H. C. Berg, Annu. Rev. Biochem. **72**, 19 (2003).
[17] P. A. Williams, S. J. Papadakis, A. M. Patel, M. R. Falvo, S. Washburn, and R. Superfine, Phys. Rev. Lett. **89**, 255502 (2002).